Supporting Information

Elongation Factor Tu's Nucleotide Binding Is Governed by a Thermodynamic Landscape Unique among Bacterial Translation Factors

Dylan Girodat†‡, Evan Mercier†‡§, Katherine E. Gzyl†, and Hans-Joachim Wieden†*

†Alberta RNA Research and Training Institute (ARRTI), Department of Chemistry and Biochemistry, University of Lethbridge, 4401 University Drive West, Lethbridge, Alberta T1K 3M4, Canada

§Present address: Department of Physical Biochemistry, Max Planck Institute of Biophysical Chemistry, Am Fassberg 11, 37077 Göttingen, Germany

‡These authors contributed equally to this work

*Corresponding author

Supplemental Discussion

Insights into the *apo* Conformation of EF-Tu

The first structural insight into the *apo* conformation of EF-Tu was gleaned from the crystal structure of the EF-Tu•EF-Ts complex[1]. In this structure, switch I of EF-Tu is disordered and the domain arrangement is similar to the GDP conformation. Subsequently, Thirup and co-workers were able to crystalize an EF-Tu•EF-Ts complex with EF-Tu in the closed GTP conformation, indicating that the EF-Tu•EF-Ts complex exhibits conformational flexibility[2]. Our kinetic data reported here provides additional insight in the *apo* state of EF-Tu and suggests that the free *apo* state of EF-Tu adopts a unique conformation that is able to recognize GTP and GDP similarly. Similar association and different dissociation activation barriers support that nucleotide binding to this non-discriminatory conformation of EF-Tu is followed by conformational changes of EF-Tu that depend on the presence and absence of the gamma-phosphate in GTP. Therefore, the nucleotide release mechanism is likely the inverse in which a conformational change has to occur prior to nucleotide dissociation. This process would require a unique conformation for EF-Tu•*apo* and is constant with the reported conformational flexibility observed by Johansen *et al* and Kavaliauskas *et al*[3-4].

Considering the entropic landscape of EF-Tu, the EF-Tu•*apo* conformation is less stable than both EF-Tu•GTP and EF-Tu•GDP (Fig 4). Since EF-Tu employs water coordination to entropically stabilize the GTP conformation it is likely that water coordination stabilizes EF-Tu•GTP and EF-Tu•GDP compared to EF-Tu•*apo*. If GDP is removed from the structure of EF-Tu•GDP the SASA increases by 109 Å^2. The difference in SASA between EF-Tu•GTP and EF-Tu•GDP is 1041 Å^2 (Fig S6B) and since the entropy gap between EF-Tu•GDP and EF-Tu•GTP is similar to the entropy gap between EF-Tu•*apo* and EF-Tu•GDP (Fig 4C) it is likely that SASA alone does not explain the entropy of the EF-Tu•*apo* conformation. Therefore, EF-Tu•*apo* cannot merely be a similar conformation to EF-Tu•GDP without nucleotide, but has to be a unique conformation. Another possible explanation for the entropy of EF-Tu•*apo* is that this state is less flexible. This is unlikely as switch I is disordered in the EF-Tu•EF-Ts crystalized complex from Kawashima *et al*[1]. If this is the conformation that switch I adopts in the *apo* state then it is likely going to be more flexible. However, this does agree with the observation that EF-Tu•*apo* coordinates more water molecules, as a disordered switch I would have a larger SASA. Since EF-Tu•*apo* is less entropically stable compared to EF-Tu•GTP or EF-Tu•GDP which cannot be explained simply by the loss of nucleotide or EF-Tu•*apo* being less flexible then EF-Tu•*apo* must adopt a unique conformation.

To directly compare the thermodynamic contributions of each nucleotide bound state relative to each other we can use the law of mass-action. However, since GTP contains an additional phosphate compared to GDP mass is not conserved in the kinetic mechanism of EF-Tu nucleotide binding, preventing the implementation of mass action (Fig 1). The fact that there is no difference in the $\Delta H^{\ddagger}_a$ or $T\Delta S^{\ddagger}_a$ and that the mass is conserved in the respective halves of the nucleotide dissociation mechanism (k_{-1} and k_{-2}), which defines the thermodynamic landscape of nucleotide binding, indicates that the mass of P_i has little to no influence

The Enthalpic Stability of EF-Tu•GDP is Targeted by EF-Ts for Nucleotide Dissociation

Since EF-Tu and EF-Ts have co-evolved, the residues involved in stabilizing the GDP conformation of EF-Tu are likely the same residues targeted by EF-Ts to help mediate GDP release. The current understanding is that EF-Ts stimulates GDP dissociation from EF-Tu through 3 factors: (1) destabilization of the Mg^{2+} coordination, (2) flipping of the P-loop and (3) destabilizing the nucleotide-ribose binding site[1, 5-6]. Previously, the interactions between EF-Ts and helix B (switch II – amino acids 84-92), as well as helix D (amino acids 139-144) have been studied as EF-Ts makes direct interactions with these regions of EF-Tu[5-9]. Crystal structures of the EF-Tu•EF-Ts complex show that residues in helix A of EF-Tu contact the C-terminal end of EF-Ts[1]. Additionally, our group has previously shown that these interactions destabilize helices A and F and increase the rate of nucleotide release 10-fold[10]. Since helix A is located in proximity to a number of interactions that stabilize the GDP conformation, it is likely that EF-Ts specifically disrupts these hydrogen bonds. Two possible mechanisms may explain how the C-terminus of EF-Ts helps to stimulate GDP dissociation: (1) it helps position EF-Ts properly onto EF-Tu in order for F81 to insert between H118 and H84 or (2) EF-Ts destabilizes the hydrogen bonding potential of helix A and as a consequence lowers the $\Delta H^{\ddagger}_d$ barrier favoring dissociation. Our data supports the latter hypothesis and is consistent with the crystal structure of the EF-Tu•GDPNP•EF-Ts complex where EF-Ts engages with EF-Tu in a conformation where the C-terminus does not pack against helix A[2]. This structural model suggests that these interactions are not required for EF-Ts binding but are, instead, involved in promoting efficient nucleotide dissociation[2].

Table S1. Temperature specific rate constants of nucleotide association and dissociation to EF-Tu. Previously reported rates for EF-Tu mant-nucleotide association and dissociation rates at 20°C are from Gromadski *et al.,* 2002[11]. K indicates in the presence of 5μM Kirromycin.

	Temperature (°C)								
	4	6	12	15	20°C[11]	22	25	29	37
mant•GDP k_{on} ($x10^6$ M^{-1} s^{-1})	0.3 ± 0.1	-	1.1 ± 0.1	-	2 ± 0.5	1.7 ± 0.1	-	2.1 ± 0.2	5.1 ± 0.3
mant•GDP k_{off} ($x10^{-3}$ s^{-1})	0.4 ± 0.1	-	0.8 ± 0.1	-	2 ± 1	1.4 ± 0.1	-	3.1 ± 0.1	7.1 ± 0.3
mant•GTP k_{on} ($x10^5$ M^{-1} s^{-1})	1.6 ± 0.1	-	2.6 ± 0.1	-	5 ± 1	4.0 ± 0.1	-	5.5 ± 0.1	9.1 ± 0.1
mant•GTP k_{off} ($x10^{-3}$ s^{-1})	-	11 ± 1	-	16 ± 1	30 ± 10	-	28 ± 4	-	60 ± 2
K mant•GDP k_{on} ($x10^6$ M^{-1} s^{-1})									3.5 ± 0.5
K mant•GDP k_{off} ($x10^{-3}$ s^{-1})									61 ± 6
K mant•GTP k_{on} ($x10^5$ M^{-1} s^{-1})									4.3 ± 0.3
K mant•GTP k_{off} ($x10^{-3}$ s^{-1})									9 ± 1

Table S2. Transition state thermodynamic properties governing nucleotide binding in EF-Tu compared to equilibrium determine thermodynamic properties. * Equilibrium values determined at 20°C by Talavera *et al*. 2018 – GTP values are for GDPγS, and K indicates in the presence of 5μM Kirromycin[12].

	$\Delta H^{\circ\ddagger}_a$ kJ/mol	$\Delta H^{\circ\ddagger}_d$ kJ/mol	ΔH°_B kJ/mol	$T\Delta S^{\circ\ddagger}_a$ kJ/mol	$T\Delta S^{\circ\ddagger}_d$ kJ/mol	$T\Delta S^{\circ}_B$ kJ/mol	$\Delta G^{\circ\ddagger}_a$ kJ/mol	$\Delta G^{\circ\ddagger}_d$ kJ/mol	ΔG°_B kJ/mol	ΔH°_B* kJ/mol	$T\Delta S^{\circ}_B$* kJ/mol	ΔG°_B* kJ/mol
GTP	36 ± 2	35 ± 1	-1 ± 3	-4 ± 2	-46 ± 1	42 ± 5	40 ± 4	81 ± 2	-41 ± 6	-5 ± 3	36 ± 1	-41 ± 1
GDP	34 ± 4	61 ± 1	-27 ± 5	3 ± 4	-27 ± 1	30 ± 5	37 ± 7	88 ± 3	-50 ± 10	-26 ± 2	21 ± 1	-46 ± 1
K GTP									-46 ± 1	-	-	-
K GDP									-47 ± 4	-	-	-

Table S3. Entropic contributions summary of the EF-Tu•GTP and EF-Tu•GDP conformations (figure 7B, C). Coordinated water molecules were determined as water within 2.5Å of EF-Tu.

EF-Tu Conformation	SASA (Å^2) mean	SASA (Å^2) Standard Deviation	# of Water Molecules mean	# of Water Molecules Standard Deviation
GTP	19357	297	318	11
GDP	20398	261	334	11

Table S4. Difference in transition state thermodynamic properties governing nucleotide dissociation for EF-Tu variants compared to wild type (TΔΔS measured at 20°C). *-values reported in Mercier *et al*[13].

	$\Delta\Delta H^{\circ\ddagger}_d$ kJ/mol	$T\Delta\Delta S^{\circ\ddagger}_d$ kJ/mol	$\Delta\Delta G^{\circ\ddagger}_d$ kJ/mol
H22G•GTP*	19 ± 4	18 ± 4	2 ± 8
H22G•GDP	-5 ± 3	2 ± 3	-7 ± 6
M112L•GTP*	1 ± 2	6 ± 2	-5 ± 5
M112L•GDP	1 ± 4	6 ± 4	-4 ± 7

Table S4. Location of waters that are resident (within 4.0Å of EF-Tu) in a single location in the EF-Tu•GTP or EF-Tu•GDP simulations during more than 50% of frames.

EF-Tu•GTP			EF-Tu•GDP		
Water Molecule ID	% of Frames	Position	Water Molecule ID	% of Frames	Position
6337	100	Mg^{2+} Coordination	6130	100	Mg^{2+} Coordination
6334	100	Mg^{2+} Coordination	6127	100	P-Loop (H22/T115/V104)
6142	100	GTP Interaction (Near G83)	6121	100	Mg^{2+} Coordination
6130	100	P-Loop (H22/H19)	6103	100	Mg^{2+} Coordination
14632	94.7	Helix D (S183/W184)	6100	100	Mg^{2+} Coordination
11764	89.0	Domain II (E243/K294/I298/T297)	6088	100	Mg^{2+} Coordination
28942	64.1	Helix D (R74/I199)	6112	99.9	Helix D (S173/W184/K187)
6136	60.8	Domain II/Switch II (I214/Q290)	47376	99.6	GDP (K24/V20)
11377	57.0	Switch II (H118/H84/Q214)	55629	91.0	Helix D (Y176/V12/I199/R74)
44749	53.8	Switch II (T64/T93/G94)	34896	67.22	Domain II (G296/T297/K294)
41926	52.6	Domain I (T167/I130/Y198)	15375	52.4	Domain II/III(R333/R230/P213)
45604	50.3	Domain III/Switch II (R333/T334/T93)			

Table S5. Summary of hydrogen bonds formed by the peptidyl backbone carboxylic acid oxygen (O) to a peptidyl backbone amide (N-H) of EF-Tu

Residue	% of frames a hydrogen bond is formed between a backbone O to a backbone N-H		% Difference (GDP-GTP)	Residue	% of frames a hydrogen bond is formed by a backbone O to a backbone N-H		% Difference (GDP-GTP)
	GTP	GDP			GTP	GDP	
1	1.21	0.01	-1.20	197	0.00	0.00	0.00
2	0.01	0.00	-0.01	198	0.00	0.00	0.00
3	77.23	0.02	-77.21	199	0.00	0.00	0.00
4	0.19	0.07	-0.12	200	0.00	0.00	0.00
5	0.06	1.67	1.61	201	0.00	0.01	0.01
6	1.96	0.00	-1.96	202	0.00	0.00	0.00
7	0.01	0.00	-0.01	203	0.00	0.12	0.12
8	0.00	0.00	0.00	204	12.39	14.74	2.36
9	0.00	0.00	0.00	205	81.96	88.79	6.83
10	88.37	81.54	-6.82	206	12.87	0.03	-12.83
11	0.00	0.00	0.00	207	0.00	0.00	0.00
12	42.80	74.47	31.67	208	0.03	0.03	0.00
13	100.59	91.67	-8.92	209	0.00	0.00	0.00
14	80.81	20.14	-60.67	210	4.47	6.98	2.51
15	92.67	84.86	-7.81	211	70.82	57.13	-13.69
16	4.78	0.00	-4.78	212	92.34	94.06	1.71
17	75.90	51.44	-24.46	213	0.00	0.00	0.00
18	0.00	0.00	0.00	214	3.76	0.00	-3.76
19	1.12	0.00	-1.12	215	29.80	0.00	-29.80
20	0.23	0.02	-0.21	216	35.69	45.04	9.36
21	0.00	0.00	0.00	217	0.00	0.01	0.01
22	0.00	0.00	0.00	218	77.17	76.61	-0.56
23	69.17	75.57	6.40	219	0.00	0.03	0.03
24	53.71	55.81	2.10	220	62.67	4.92	-57.74
25	58.71	60.40	1.69	221	10.26	0.13	-10.12
26	56.61	78.68	22.07	222	0.00	0.70	0.70
27	90.84	95.14	4.30	223	0.00	14.30	14.30
28	20.06	3.98	-16.08	224	57.54	24.22	-33.32
29	17.53	25.87	8.33	225	60.78	53.61	-7.17
30	48.03	84.00	35.97	226	81.29	73.56	-7.73
31	31.99	39.21	7.22	227	79.58	88.17	8.59
32	32.83	43.52	10.69	228	91.43	79.98	-11.46
33	47.01	57.50	10.49	229	78.10	65.29	-12.81
34	48.90	60.77	11.87	230	0.01	0.27	0.26
35	70.67	93.54	22.88	231	91.80	84.21	-7.59
36	29.80	0.87	-28.93	232	0.00	0.00	0.00
37	0.21	0.00	-0.21	233	66.82	51.80	-15.02

38	0.18	0.00	-0.18	234	27.71	16.60	-11.11
39	0.00	0.00	0.00	235	0.09	0.02	-0.07
40	0.04	0.09	0.04	236	70.03	77.52	7.49
41	0.62	0.09	-0.53	237	0.32	0.66	0.33
42	7.73	0.12	-7.61	238	1.30	3.87	2.57
43	0.03	0.00	-0.03	239	0.00	0.00	0.00
44	0.97	0.01	-0.96	240	80.53	72.02	-8.51
45	16.81	3.20	-13.61	241	0.00	0.00	0.00
46	56.29	97.14	40.86	242	63.71	54.27	-9.44
47	0.26	47.90	47.64	243	70.54	88.99	18.44
48	0.00	0.07	0.07	244	0.06	7.43	7.38
49	0.02	0.01	-0.01	245	17.57	46.74	29.18
50	0.02	22.50	22.48	246	0.00	20.36	20.36
51	0.00	0.00	0.00	247	0.23	0.00	-0.23
52	28.76	0.00	-28.76	248	0.27	0.04	-0.22
53	30.53	7.03	-23.50	249	0.02	0.76	0.73
54	36.70	0.04	-36.66	250	0.73	0.00	-0.73
55	33.93	72.44	38.51	251	77.40	88.71	11.31
56	0.91	1.02	0.11	252	0.00	0.00	0.00
57	0.00	7.50	7.50	253	80.41	75.20	-5.21
58	9.06	19.29	10.23	254	11.38	41.43	30.06
59	0.00	0.00	0.00	255	69.37	71.23	1.87
60	0.01	37.36	37.34	256	0.00	0.00	0.00
61	0.00	0.00	0.00	257	82.76	80.90	-1.86
62	0.00	83.49	83.49	258	34.41	86.09	51.68
63	0.00	0.00	0.00	259	90.06	80.60	-9.46
64	0.01	0.24	0.23	260	8.39	0.96	-7.43
65	67.28	37.21	-30.07	261	0.00	0.00	0.00
66	0.00	0.00	0.00	262	0.00	0.00	0.00
67	92.04	82.22	-9.82	263	76.74	20.27	-56.48
68	0.00	0.00	0.00	264	75.58	0.00	-75.58
69	86.28	93.29	7.01	265	0.00	21.99	21.99
70	0.01	0.01	0.00	266	0.02	14.76	14.73
71	0.36	0.28	-0.08	267	0.62	0.04	-0.58
72	0.00	0.00	0.00	268	73.78	69.17	-4.61
73	0.00	0.00	0.00	269	12.13	9.58	-2.56
74	46.88	54.87	7.99	270	1.97	0.17	-1.80
75	38.80	81.66	42.86	271	0.00	0.04	0.04
76	20.79	38.18	17.39	272	38.79	60.31	21.52
77	88.12	70.77	-17.36	273	0.00	0.00	0.00
78	63.57	61.88	-1.69	274	15.10	22.40	7.30
79	18.14	22.24	4.10	275	66.58	84.68	18.10
80	27.26	76.31	49.06	276	59.89	82.69	22.80

81	0.00	0.03	0.03	277	76.62	86.39	9.77
82	0.00	0.00	0.00	278	13.88	16.57	2.69
83	14.34	13.07	-1.28	279	50.97	9.16	-41.81
84	5.37	46.41	41.04	280	0.01	0.00	-0.01
85	0.41	59.43	59.02	281	0.02	4.14	4.12
86	14.18	50.62	36.44	282	33.41	8.83	-24.58
87	5.66	69.76	64.10	283	2.52	9.43	6.91
88	68.42	49.17	-19.26	284	0.00	0.03	0.03
89	20.67	69.97	49.30	285	0.01	0.71	0.70
90	13.64	6.44	-7.20	286	0.00	0.00	0.00
91	100.00	0.00	-100.00	287	0.08	0.13	0.06
92	42.63	0.13	-42.50	288	1.01	0.00	-1.01
93	0.32	0.31	-0.01	289	0.00	0.00	0.00
94	29.59	2.67	-26.92	290	86.70	36.88	-49.82
95	13.29	0.02	-13.27	291	78.53	70.72	-7.81
96	0.00	0.03	0.03	292	67.92	86.02	18.10
97	0.00	0.02	0.02	293	89.27	84.69	-4.58
98	0.00	0.00	0.00	294	0.64	0.34	-0.30
99	1.34	1.13	-0.21	295	0.34	0.07	-0.28
100	1.93	0.68	-1.26	296	0.00	0.00	0.00
101	67.96	54.16	-13.80	297	0.01	0.00	-0.01
102	70.24	71.14	0.90	298	0.00	0.00	0.00
103	85.22	89.09	3.87	299	0.21	9.04	8.83
104	0.00	0.00	0.00	300	0.00	0.00	0.00
105	98.70	97.48	-1.22	301	56.88	50.76	-6.12
106	67.37	50.23	-17.13	302	63.14	70.27	7.12
107	0.00	0.00	0.00	303	59.50	56.06	-3.44
108	0.00	0.00	0.00	304	86.66	86.84	0.19
109	0.00	0.00	0.00	305	87.28	84.62	-2.66
110	3.21	1.32	-1.89	306	63.20	61.72	-1.48
111	0.00	0.00	0.00	307	38.57	42.24	3.68
112	49.71	41.34	-8.37	308	46.94	73.92	26.98
113	44.08	57.74	13.67	309	76.81	57.22	-19.59
114	66.96	60.49	-6.47	310	24.31	61.01	36.70
115	1.92	3.04	1.12	311	16.93	0.31	-16.62
116	20.09	39.31	19.22	312	83.04	93.72	10.68
117	95.74	86.03	-9.71	313	1.86	2.97	1.11
118	67.49	50.40	-17.09	314	0.01	0.01	0.00
119	37.71	40.49	2.78	315	0.09	0.00	-0.09
120	47.97	53.08	5.11	316	0.63	2.29	1.66
121	89.57	67.08	-22.49	317	0.02	0.00	-0.02
122	85.46	100.00	14.54	318	0.16	1.13	0.98
123	0.34	0.17	-0.18	319	0.00	0.00	0.00

124	0.00	0.00	0.00	320	0.00	0.00	0.00
125	0.00	0.00	0.00	321	0.21	0.00	-0.21
126	0.00	0.00	0.00	322	75.17	82.58	7.41
127	0.19	0.00	-0.19	323	3.18	5.54	2.37
128	0.61	5.64	5.03	324	1.27	6.37	5.10
129	61.30	41.51	-19.79	325	0.00	0.00	0.00
130	0.00	0.00	0.00	326	27.53	2.96	-24.58
131	93.10	91.78	-1.32	327	0.00	0.00	0.00
132	46.34	60.49	14.14	328	8.67	23.31	14.64
133	47.54	53.44	5.90	329	57.89	79.08	21.19
134	79.70	81.29	1.59	330	51.87	46.08	-5.79
135	87.61	88.71	1.10	331	49.81	42.76	-7.06
136	17.66	18.28	0.62	332	0.12	9.61	9.49
137	1.13	0.42	-0.71	333	0.00	0.01	0.01
138	0.00	0.00	0.00	334	0.00	0.00	0.00
139	0.13	0.24	0.11	335	10.31	25.51	15.20
140	0.00	0.00	0.00	336	0.00	0.06	0.06
141	0.03	0.02	-0.01	337	94.16	97.00	2.84
142	11.76	11.40	-0.36	338	35.83	2.02	-33.81
143	51.93	54.37	2.43	339	0.06	0.01	-0.04
144	35.02	31.78	-3.24	340	49.77	66.37	16.60
145	46.82	40.70	-6.12	341	30.50	0.06	-30.44
146	38.81	50.89	12.08	342	50.54	57.03	6.49
147	46.83	51.18	4.34	343	0.00	0.00	0.00
148	26.24	31.69	5.44	344	3.61	3.79	0.18
149	30.44	26.38	-4.07	345	5.08	4.16	-0.92
150	54.06	65.32	11.27	346	0.01	0.12	0.11
151	36.56	62.02	25.47	347	0.00	0.00	0.00
152	28.50	32.59	4.09	348	7.58	6.77	-0.81
153	56.58	62.39	5.81	349	1.09	0.24	-0.84
154	47.07	56.88	9.81	350	22.52	31.14	8.62
155	46.87	28.91	-17.96	351	1.82	0.59	-1.23
156	11.99	4.82	-7.17	352	3.96	0.84	-3.11
157	60.80	26.60	-34.20	353	0.00	0.00	0.00
158	10.04	1.01	-9.03	354	14.76	31.93	17.18
159	4.69	0.54	-4.14	355	0.00	0.00	0.00
160	3.79	8.74	4.96	356	75.98	66.42	-9.56
161	0.00	0.00	0.00	357	0.00	0.00	0.00
162	6.47	1.97	-4.50	358	84.24	79.26	-4.99
163	29.71	18.30	-11.41	359	80.16	76.91	-3.24
164	0.17	0.19	0.02	360	53.37	49.69	-3.68
165	0.93	1.18	0.24	361	72.23	46.26	-25.98
166	0.00	0.00	0.00	362	0.00	0.00	0.00

167	0.19	0.20	0.01	363	0.00	0.00	0.00
168	23.13	35.24	12.11	364	0.03	0.31	0.28
169	0.00	0.00	0.00	365	0.00	21.94	21.94
170	94.14	96.98	2.83	366	79.88	76.21	-3.67
171	0.00	0.00	0.00	367	0.01	0.00	-0.01
172	28.33	23.53	-4.80	368	0.19	7.13	6.94
173	1.72	1.99	0.27	369	0.20	0.29	0.09
174	23.10	53.31	30.21	370	3.62	1.96	-1.67
175	61.49	59.64	-1.84	371	0.01	0.04	0.03
176	41.96	99.08	57.12	372	54.11	60.94	6.83
177	0.03	0.23	0.20	373	0.00	0.00	0.00
178	1.04	0.00	-1.04	374	28.54	50.63	22.09
179	0.16	0.00	-0.16	375	89.18	90.46	1.28
180	2.29	0.01	-2.28	376	82.00	94.09	12.09
181	29.60	54.92	25.32	377	26.76	69.16	42.40
182	36.96	34.46	-2.50	378	15.82	1.82	-14.00
183	9.67	6.93	-2.73	379	0.46	0.88	0.42
184	6.08	6.24	0.17	380	0.00	0.00	0.00
185	57.09	41.60	-15.49	381	58.27	57.03	-1.23
186	70.92	65.61	-5.31	382	0.03	0.00	-0.03
187	49.54	49.24	-0.30	383	48.78	50.62	1.84
188	74.81	67.53	-7.28	384	90.50	89.48	-1.02
189	59.34	56.07	-3.28	385	87.06	91.74	4.69
190	53.47	46.24	-7.22	386	72.61	63.10	-9.51
191	85.66	72.19	-13.47	387	51.16	39.21	-11.94
192	32.72	23.12	-9.60	388	0.00	19.78	19.78
193	54.11	56.12	2.01	389	0.00	0.00	0.00
194	80.98	69.36	-11.62	390	86.87	84.22	-2.64
195	9.22	0.30	-8.92	391	0.00	0.00	0.00
196	0.02	0.00	-0.02	392	0.00	0.00	0.00

Table S6. The modulation of *E. coli* EF-Tu nucleotide binding kinetics by antibiotics. Values determined by * - Fasano *et al*. 1978 , †- Anborgh *et al*. 1993, £ - Anborgh *et al*. 2004, and ℓ Cetin *et al*. 1996[14-17].

Antibiotic	GTP on rate (s^{-1} M^{-1})	GTP off rate (s^{-1})	GTP Affinity (nM)	GDP on rate (s^{-1} M^{-1})	GDP off rate (s^{-1})	GDP Affinity (nM)	Temp. (°C)
No antibiotic	$1.6 \pm 0.1 \times 10^{5}$	$1.1 \pm 0.1 \times 10^{-2}$	60	$0.3 \pm 0.1 \times 10^{6}$	$0.4 \pm 0.1 \times 10^{-3}$	1	4
No antibiotic*	1.0×10^{4}	5.9×10^{-3}	590	2.6×10^{5}	2.3×10^{-4}	0.9	0
Kirromycin*	1.2×10^{5}	1.7×10^{-4}	1.4	9.0×10^{5}	7.4×10^{-4}	0.8	0
GE2270 A †	1.3×10^{4}	0.15×10^{-4}	1.2	3.5×10^{5}	2.3×10^{-4}	0.7	0
Pulvomycin£	5.1×10^{4}	0.3×10^{-4}	0.6	6.0×10^{5}	5.9×10^{-5}	9.8	0
Enacyloxin IIaℓ	3.9×10^{5}	2.8×10^{-4}	0.7	7.8×10^{4}	6.2×10^{-4}	8	0

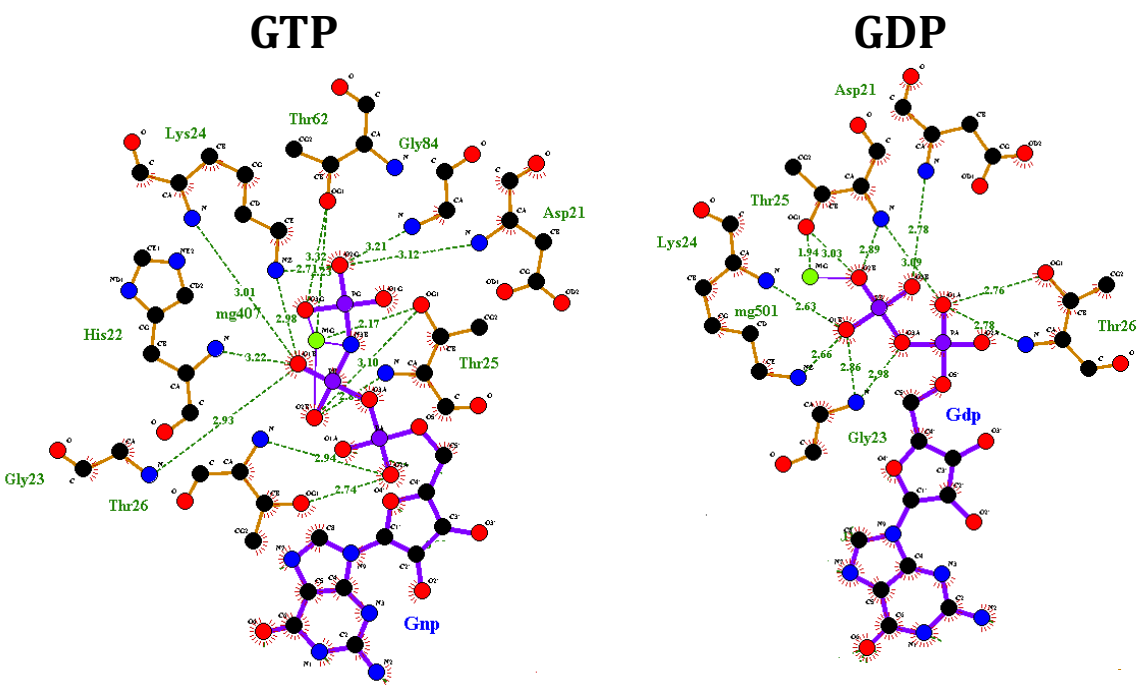

Figure S1 LIGPLOT view of EF-Tu interactions with GTP and GDP[18].

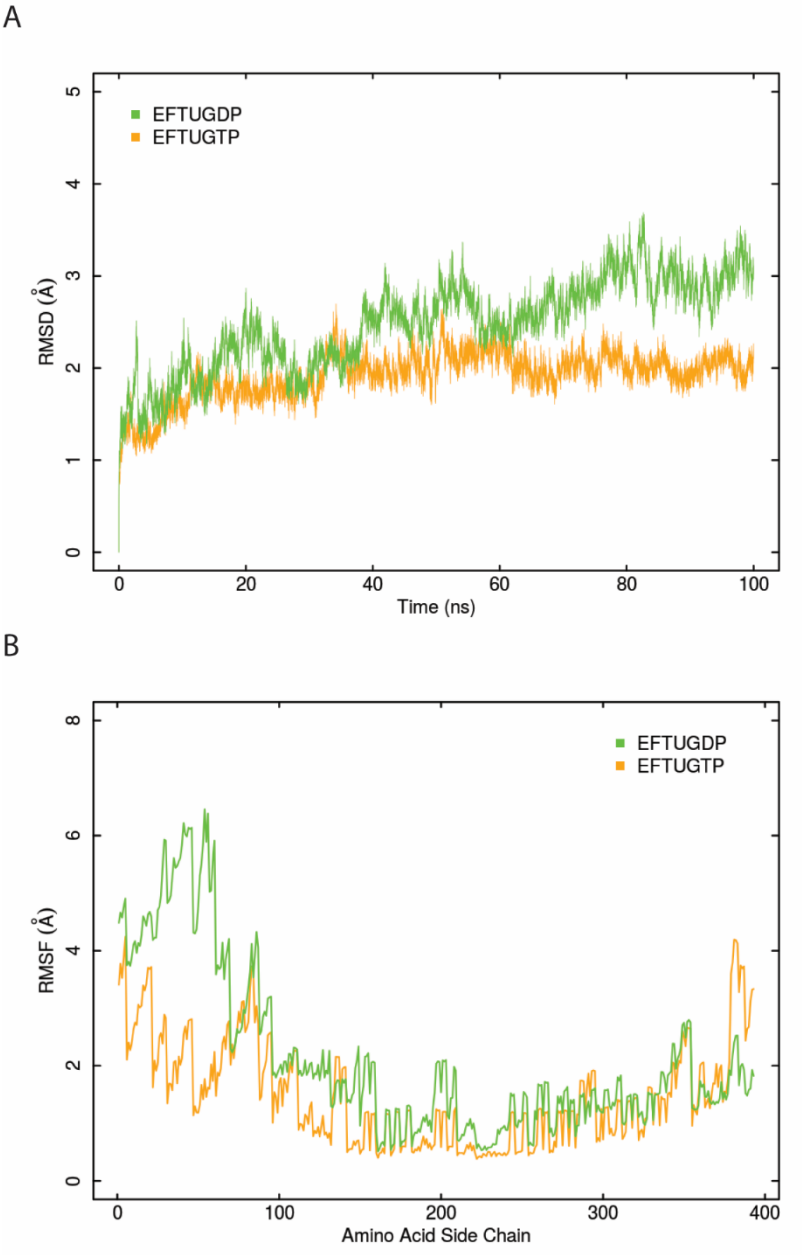

Figure S2. EF-Tu simulation deviations and flexibility (A) Root Mean Square Deviation (RMSD) and (B) Side chain Root Mean Square Fluctuation (RMSF) of the 100ns EF-Tu•GTP and EF-Tu•GDP simulations.

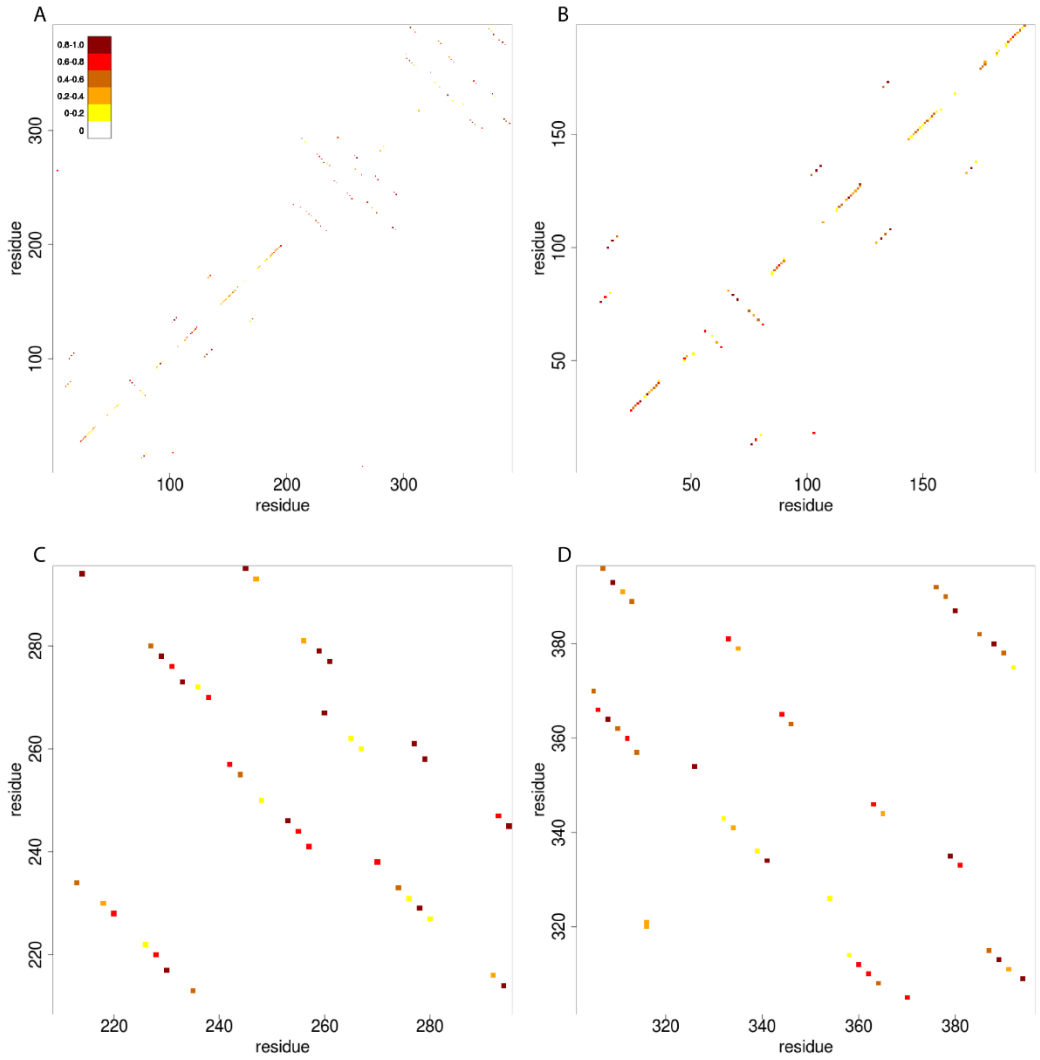

Figure S3. Hydrogen bonding network of EF-Tu•GDP. Hydrogen bonds were defined as Carboxyl O or Amide N-H of the peptide backbone that were in 3.0Å and within 60° of each other. Hydrogen bonding network of (A) EF-Tu•GDP, (B) domain I, (C) domain II, and (D) domain III. α-helices and β-strands are represented as consecutive hydrogen bonds along the bottom left to top right or top left to bottom right diagonals respectively

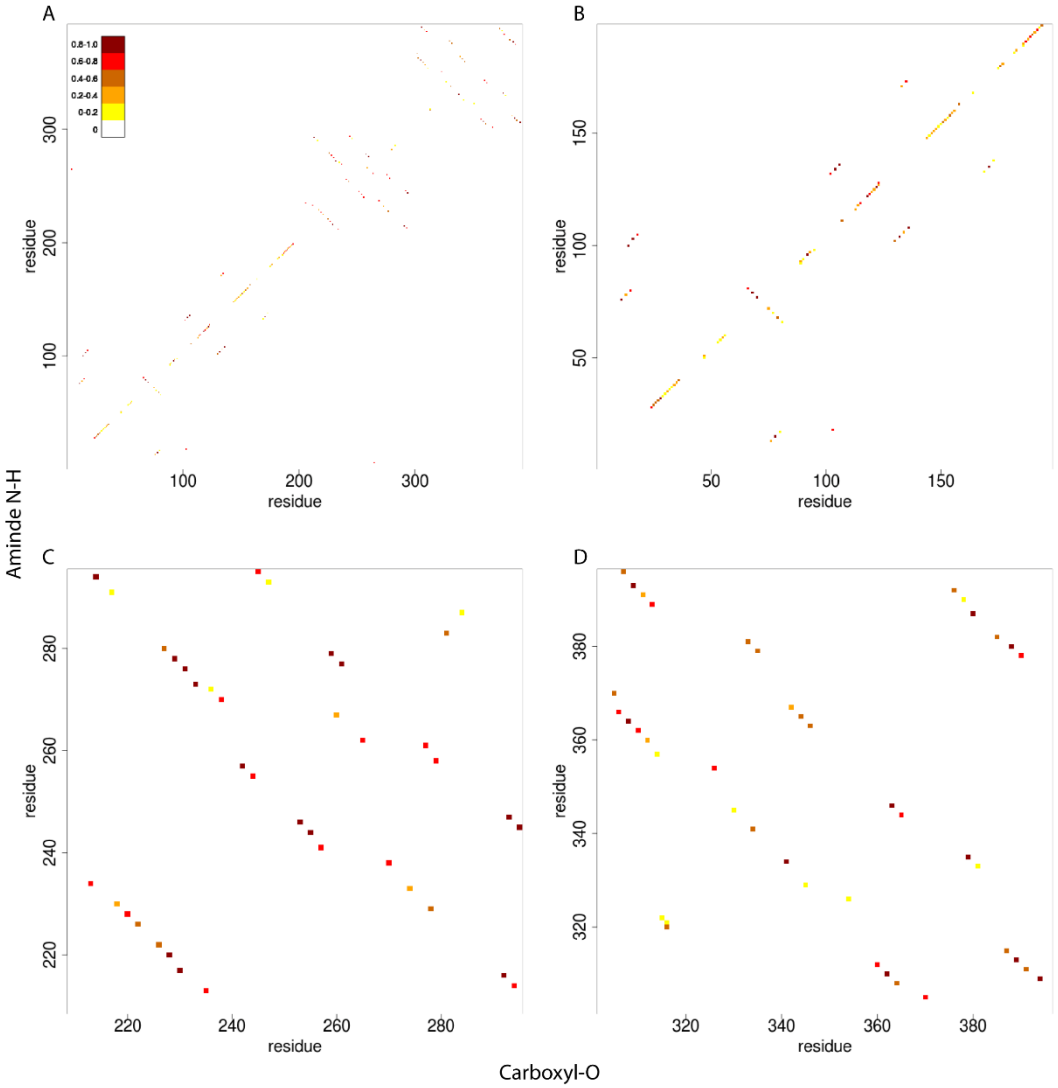

Figure S4. Hydrogen bonding network of EF-Tu•GTP. Hydrogen bonds were defined as Carboxyl O or Amide N-H of the peptide backbone that were in 3.0Å and within 60° of each other. Hydrogen bonding network of (A) EF-Tu•GTP, (B) domain I, (C) domain II, and (D) domain III. α-helices and β-strands are represented as consecutive hydrogen bonds along the bottom left to top right or top left to bottom right diagonals respectively

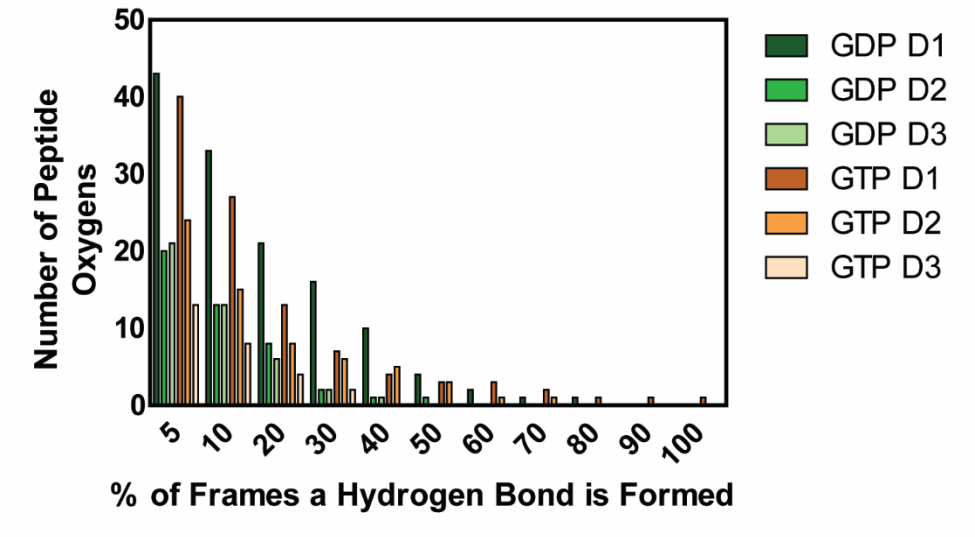

Figure S5. Number of backbone oxygens that are involved in hydrogen bonds in the EF-Tu•GTP and EF-Tu•GDP 100ns simulations separated into each domain.

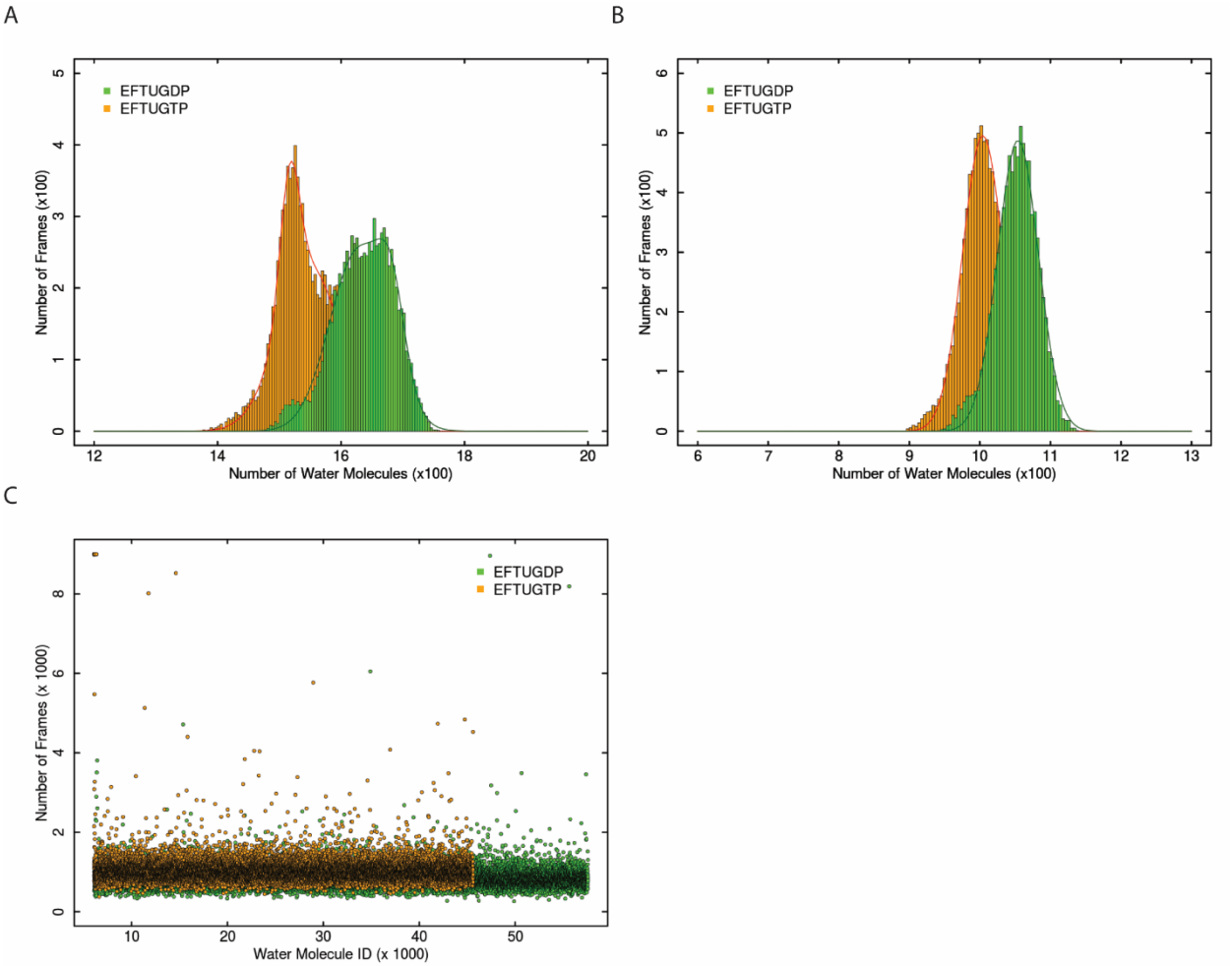

Figure S6 Water coordination of EF-Tu•GTP and EF-Tu•GDP during 100ns of simulation. (A) Water within 4.0 Å of EF-Tu (EF-Tu•GTP mean-1517 ± 16 and 1550 ± 50; EF-Tu•GDP mean-1628 ± 79 and 1682 ± 22). (B) Water within 3.0 Å of EF-Tu (EF-Tu•GTP mean – 1004 ± 29; EF-Tu•GDP mean – 1054 ± 29). (C) Residency times of water molecules in the EF-Tu simulations.

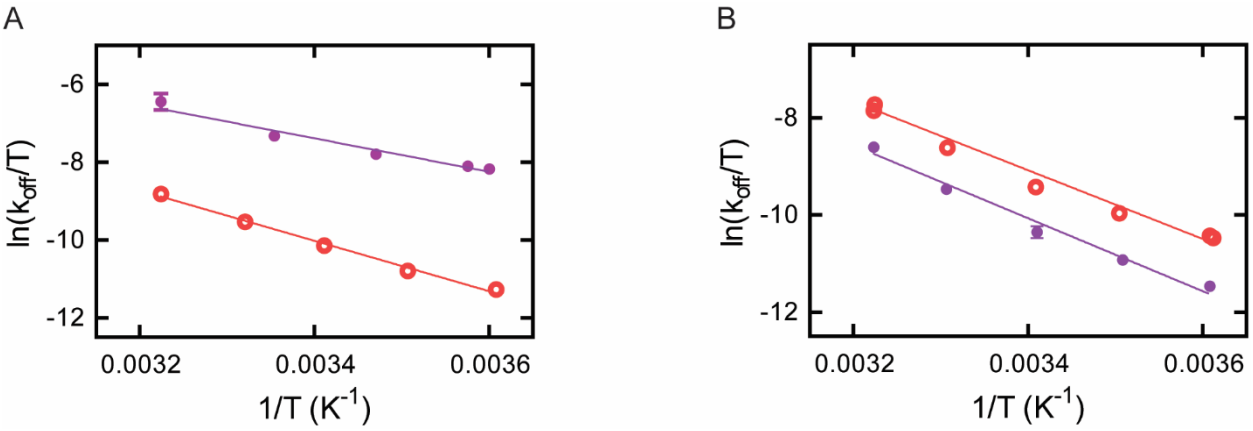

Figure S7. Eyring plot of nucleotide dissociation for EF-Tu variants H22G and M112L. (A) GTP and (B) GDP dissociation at temperatures ranging from 4°C to 37°C, M112L – purple (closed circle), H22G – red (open circle).

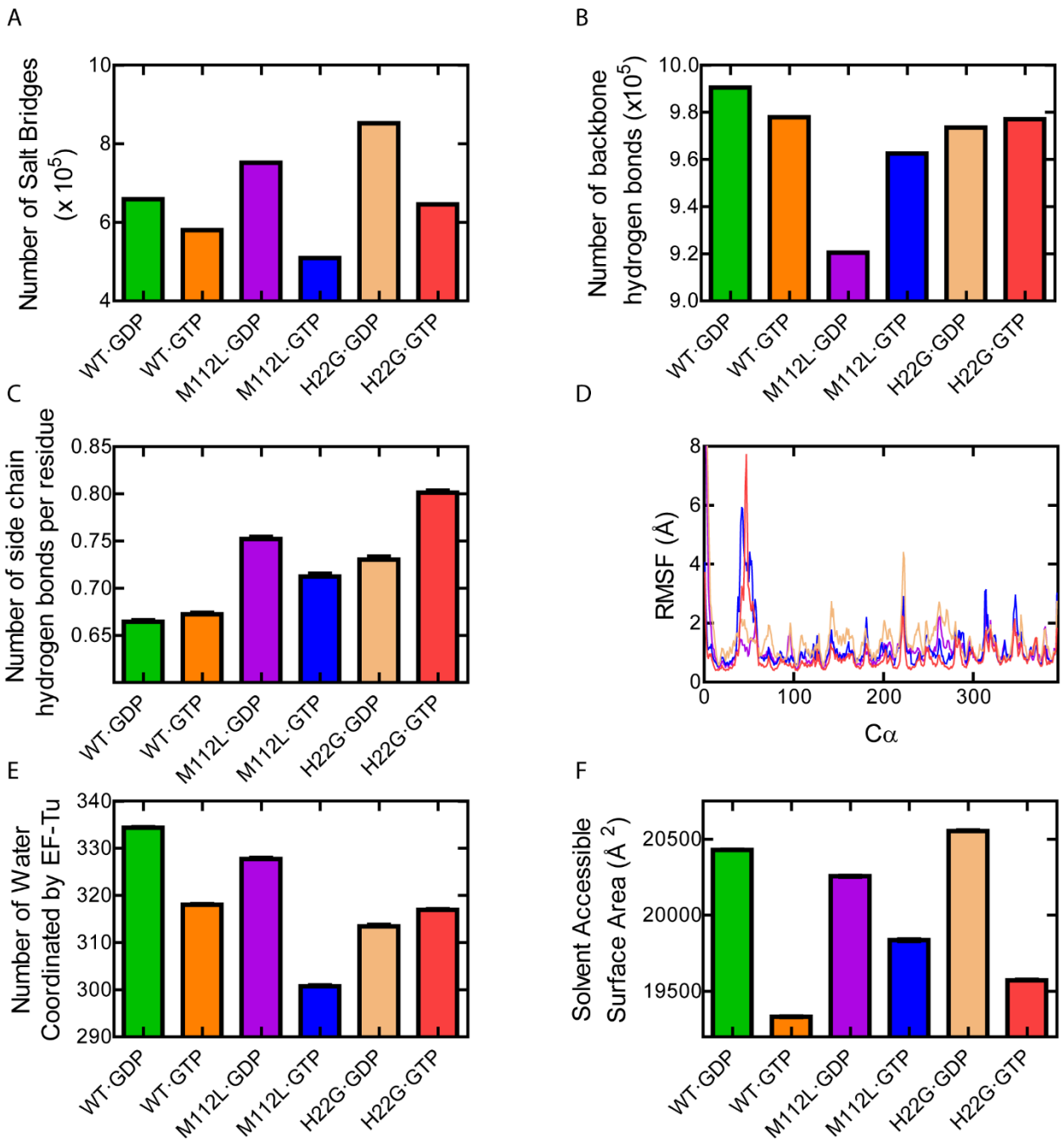

Figure S8. Analysis of 100ns EF-Tu H22G and M112L MD simulations. Enthalpic contributions to EF-Tu measured as number of (A) salt bridges, (B) backbone hydrogen bonds, and (C) sidechain hydrogen bonds in 100ns of simulation. Entropic contributions ot EF-Tu measured as (D) RMSF, (E) Number of water coordinate by EF-Tu, and (F) Solvent accessible surface area of EF-Tu. EF-Tu•GDP – green, EF-Tu•GTP – orange, M112L•GDP - purple, M112L•GTP – blue, H22G•GDP – beige, and H22G•GTP – red.

References

1. Kawashima, T.; Berthet-Colominas, C.; Wulff, M.; Cusack, S.; Leberman, R., The structures of the *Escherichia coli* EF-Tu EF-Ts complex at 2.5 Å resolution. *Nature* **1996,** *379* (8), 511-518.
2. Thirup, S. S.; Van, L. Bich; Nielsen, T. K.; Knudsen, C. R., Structural outline of the detailed mechanism for elongation factor Ts-mediated guanine nucleotide exchange on elongation factor Tu. *Journal of Structural Biology* **2015,** *191*, 10-21.
3. Johansen, J. S.; Kavaliauskas, D.; Pfeil, S. H.; Blaise, M.; Cooperman, B. S.; Goldman, Y. E.; Thirup, S. S.; Knudsen, C. R., *E. coli* elongation factor Tu bound to a GTP analogue displays an open conformation equivalent to the GDP-bound form. *Nucleic Acids Res* **2018,** *46* (16), 8641-8650.
4. Kavaliauskas, D.; Chen, C.; Liu, W.; Cooperman, B. S.; Goldman, Y. E.; Knudsen, C. R., Structural dynamics of translation elongation factor Tu during aa-tRNA delivery to the ribosome. *Nucleic Acids Res* **2018,** *46* (16), 8651-8661.
5. Wieden, H. J.; Gromadski, K.; Rodnin, D.; Rodnina, M. V., Mechanism of Elongation Factor (EF)-Ts-catalyzed nucleotide exchange in Ef-Tu. *J. Biol. Chem.* **2002,** *277* (8), 6032-6036.
6. Schümmer, T.; Gromadski, K. B.; Rodnina, M. V., Mechanism of EF-Ts-catalyzed guanine nucleotide exchange in EF-Tu: Contribution of interactions mediated by helix B of EF-Tu. *Biochemistry* **2007,** *46* (17), 4977-4984.
7. Zhang, Y. L.; Li, X.; Spremulli, L. L., Role of the conserved aspartate and phenylalanine residues in prokaryotic and mitochondrial elongation factor Ts in guanine nucleotide exchange. *FEBS* **1996,** *391* (3), 330-332.
8. Jonák, J.; Anborgh, P. H.; Parmeggiani, A., Interaction of EF-Tu with EF-Ts: substitution of His-118 in EF-Tu destabilizes the EF-Tu•EF-Ts complex but does not prevent EF-Ts from stimulating the release of EF-Tu-bound GDP. *FEBS* **1998,** *422*, 189-192.
9. Wieden, H. J.; Mercier, E.; Gray, J.; Steed, B.; Yawney, D., A combined molecular dynamics and rapid kinetics approach to identify conserved three-dimensional communication networks in elongation factor Tu. *Biophys. J.* **2010,** *99*, 3735-3743.
10. De Laurentiis, E. I.; Mercier, E.; Wieden, H. J., The C-terminal Helix of Pseudomonas aeruginosa Elongation Factor Ts Tunes EF-Tu Dynamics to Modulate Nucleotide Exchange. *J Biol Chem* **2016,** *291* (44), 23136-23148.
11. Gromadski, K. B.; Wieden, H. J.; Rodnina, M. V., Kinetic mechanism of elongation factor Ts-catalyzed nucleotide exchange in elongation factor Tu. *Biochemistry* **2002,** *41* (1), 162-9.
12. Talavera, A.; Hendrix, J.; Versées, W.; Jurénas, D.; Nerom, K. Van; Vandenberk, N.; Singh, R. Kumar; Konijnenberg, A.; Gieter, S. De; Castro-Roa, D.; Barth, A.; Greve, H. De; Sobott, F.; Hofkens, J.; Zenkin, N.; Loris, R.; Garcia-Pino, A., Phosphorylation decelerates conforational dynamics in bacterial translation elongation factors. *Science Advances* **2018,** *4*, 1-14.
13. Mercier, E.; Girodat, D.; Wieden, H. J., A conserved P-loop anchor limits the structural dynamics that mediate nucleotide dissociation in EF-Tu. *Sci. Rep.* **2015,** *5*, 7677.
14. Fasano, O.; Bruns, W.; Crechet, J. B.; Sander, G.; Parmeggiani, A., Modification of Elongation-Factor-Tu Guanine Nucleotide Interaction by Kirromycin. *Eur. J. Biochem.* **1978,** *89*, 557-565.
15. Anborgh, P. H.; Okamura, S.; Parmeggiani, A., Effects of the Antibiotic Pulvomycin on the Elongation Factor Tu-Dependent Reactions. Comparison with Other Antibiotics. *Biochemistry* **2004,** *43*, 15550-15556.
16. Cetin, R.; Krab, I. M.; Anborgh, P. H.; Cool, R. H.; Watanabe, T.; Sugyama, T.; Izaki, K.; Parmeggiani, A., Enacyloxin Ila, an inhibitor of protein biosynthesis that acts on elongation factor Tu and the ribosome. *EMBO J.* **1996,** *15* (10), 2604-2611.
17. Anborgh, P. H.; Parmeggiani, A., Probing the reactivity of the GTP- and GDP-bound conformations of Elongation Factor Tu in complex with the antibiotic GE2270 A. *J. Biol. Chem.* **1993,** *268* (33), 24622-24628.
18. Wallace, A. C.; Laskowski, R. A.; Thornton, J. M., LIGPLOT: a program to generate schematic diagrams of protein-ligand interactions. *Protein Eng.* **1995,** *8* (2), 127-134.